

Once again we thank the reviewers for comments and suggested improvements. The final version of the submitted manuscript and track version do not exactly match because the tracked version does not include the final set of the improvements. Nevertheless we match the reviewer's comments according to the both versions. We also made a number of minor grammatical corrections. Our replies marked in blue.

Abstract

Thank you for adding some concrete results here. I would make a further suggestion, however: increasing the total amount of simulated carbon can be easily achieved in many ways (for example, change the decomposition rate), however the key thing is that it is simulated in the right places. Therefore I would suggest you also add something along the lines of – the spatial correlation of the simulated and observed distribution of carbon is increased from x to y?

Done. Line 18-20

Introduction

Line 22: "and emissions to amplify climate warming" -> "and emissions that amplify climate warming"

Done. Line 24.

Line 40: Typo: Hugeluis -> Hugelius

Corrected everywhere in the manuscript.

Line 44-45: Deleted either 'area' or 'extent'

Done. Line 46.

Line 71: "an SOL" -> "a SOL"

Done. Line 76.

Last paragraph is much better. One minor comment is that it just says the aim is “to reduce the bias of initial permafrost carbon stocks” - but as you have discussed in the preceding paragraphs, improving the thermal dynamics not only improves the initial carbon stocks but the response to warming. So perhaps change this to “to reduce the bias of initial permafrost carbon stocks and improve the dynamics”

We reworded the text.

Methods

Move lines 215 - 223 (until end of sentence) to the next section as they are about the roots. Lines 267-270. The following is basically a repeat of the previous paragraph:

"We restricted simulated root growth to occur only in thawed soil layers. In SiBCASA, leaf growth is linked to fine root growth (Schaefer et al., 2008), so this also delays spring leafout until the soil begins to thaw. We first calculated the fraction of thawed roots within the root zone defined by:"

I suggest to change it to

"In order to restrict simulated root growth to thawed soil layers, we first calculated the fraction of thawed roots within the root zone defined by:"

Done. Lines 242-250.

Results

Lines 370-394: Paragraph on vertical profiles. Discusses what the modelled profiles are but does not compare to measured ones. Harden et al. 2012 (which is referenced, but not discussed) shows some observed profiles. I suggest to add one or two sentences along the lines of: The carbon in the active layer below the organic layer is lower than in the observed profiles in Harden et al. This is probably because cryoturbation is not included in the model. The top SOL and deeper carbon match well with the observed profiles (?).

Done. Lines 331-333.

Lines 405-433: Final paragraph of results. Discusses new initialisation. This paragraph is not totally clear. I am a bit confused by this sentence: "However, the NCSCD map (Fig 6B) shows that not all permafrost regions contain a uniform amount of frozen carbon." Would we expect them to? How discusses the differences between NCSCD and the simulation, but it would be good to indicate actually how much the distribution is improved by initialising with the NCSCD rather than the original method. For this I would suggest to make a spatial correlation of the NCSCD with your simulations. This value can then go into the conclusion and abstract as well.

Lines 352-355. Now it read as: The spatial correlation between simulated and observed permafrost carbon is 0.63 when initializing with the NCSCD (Fig 6b), compared with a spatial correlation of 0.12 for the uniform permafrost carbon density (Fig 6a). The amount and spatial distribution of permafrost carbon significantly improves when initializing with NCSCD.

Discussion

Lines 489-492: Seems to suggest that when the carbon is below the active layer it does not influence the soil thermal dynamics. Does it not still change the thermal properties of the permafrost, and because this part of the soil column is thermally connected to the active layer part above it, it should have at least a small influence on the active layer thermal dynamics?

Lines 391-393: The carbon content does influence thermodynamic properties of the permafrost and we now see that this statement was misleading, so we removed the active layer carbon dynamics from the statement. Now it read as: Consequently, the ALT does not change between simulations and the volume of permafrost in the top three meters of soil does not change as well.

Line 556: 'SND' -> 'SD'?

Fixed in the current version

Lines 505-561. This is interesting but I'm not sure it is completely relevant. I realise this was added on my suggestion, but the reason I suggested it was because you were saying that permafrost was or wasn't simulated in particular regions due to meteorological variables / snow, and my concern was that those assertions shouldn't be made without showing something more concrete. However, now those original comments are not in the manuscript I think it might be better to remove this paragraph? But I leave it up to you to decide.

We decided to keep the material in the manuscript, but shortened the text to maintain a smooth flow. Lines 419-436

Conclusion

As I have mentioned in the comments for the abstract/results, it would be really good to say something about the spatial distribution improving as well as increasing the amount of carbon simulated.

Lines 450-453. Now reads: Our model developments improved both the total amount and the spatial distribution of simulated permafrost carbon. The total permafrost carbon increasing from 313 Gt C to 560 Gt C, compared to the observed value of 550 Gt C, and the spatial correlation with the observed distribution increased from 0.12 to 0.63. These improvements indicate the importance of including these developments in all land surface models.

I also suggest that you add a sentence along the lines of 'These improvements indicate the importance of including these developments in all land surface models.'

Line 619 : 'modified' -> 'modify'

Done

The importance of a surface organic layer in simulating permafrost thermal and carbon dynamics

Elchin Jafarov^{1*} and Kevin Schaefer²

¹Institute of Arctic and Alpine Research, University of Colorado at Boulder, Boulder, CO 80309

²National Snow and Ice Data Center, Cooperative Institute for Research in Environmental Sciences, University of Colorado at Boulder, Boulder, CO 80309

*Corresponding author, Email: elchin.jafarov@colorado.edu

Abstract

Permafrost-affected soils contain twice as much carbon as currently exists in the atmosphere. Studies show that warming of the perennially frozen ground could initiate significant release of the frozen soil carbon into the atmosphere. Initializing the frozen permafrost carbon with the observed soil carbon distribution from the Northern Circumpolar Soil Carbon Dataset reduces the uncertainty associated with the modeling of the permafrost carbon feedback. To improve permafrost thermal and carbon dynamics we implemented a dynamic surface organic layer with vertical carbon redistribution, and introduced dynamic root growth controlled by active layer thickness, which improved soil carbon exchange between frozen and thawed pools. These changes increased the initial amount of simulated frozen carbon from 313 to 560 GtC, consistent with observed frozen carbon stocks, and increased the spatial correlation of the simulated and observed distribution of frozen carbon from 0.12 to 0.63.

1. Introduction

Warming of the global climate will lead to widespread permafrost thaw and degradation with impacts on ecosystems, infrastructure, and emissions that amplify climate warming (Oberman,

Kevin Schaefer 2/2/2016 11:25 AM

Deleted: To reduce the uncertainty associated with the modeling of the permafrost carbon feedback it is important to start with the observed soil carbon distribution.

Kevin Schaefer 2/2/2016 11:25 AM

Deleted: We initialized frozen carbon using the recent Northern Circumpolar Soil Carbon Dataset.

Kevin Schaefer 2/2/2016 11:25 AM

Deleted: better address

Kevin Schaefer 2/2/2016 11:28 AM

Deleted: These changes increased the amount of simulated frozen carbon for present conditions from 313 to 560 GtC, which is more consistent with the observed frozen carbon stock. The spatial correlation of the simulated and observed distribution of frozen carbon is increased from 0.12 to 0.63.

Elchin Jafarov 1/30/2016 11:01 AM

Deleted: to

40 2008; Callaghan et al., 2011, Shuur et al., 2015). Permafrost-affected soils in the high northern
41 latitudes contain 1300 ± 200 Gt of carbon, where ~ 800 Gt C is preserved frozen in permafrost
42 with ~ 550 GtC in the top three meters of soil (Hugelius et al., 2014). As permafrost thaws,
43 organic matter frozen within permafrost will thaw and decay, which will initiate the permafrost
44 carbon feedback (PCF), releasing an estimated 120 ± 85 Gt of carbon emissions by 2100
45 (Schaefer et al., 2014). The wide range of estimates of carbon emissions from thawing
46 permafrost depends in large part on the ability of models to simulate present permafrost extent
47 (Brown et al., 1997). For example, the simulated permafrost in some models is significantly
48 more sensitive to thaw, with corresponding larger estimates of carbon emissions (Koven et al.,
49 2013). Narrowing the uncertainty in estimated carbon emissions requires improvements in how
50 Land Surface Models (LSMs) represent permafrost thermal and carbon dynamics.

51 The active layer in permafrost regions is the surficial soil layer overlying the permafrost,
52 which undergoes seasonal freeze-thaw cycles. Active layer thickness (ALT) is the maximum
53 depth of thaw at the end of summer. LSMs used to estimate emissions from thawing permafrost
54 typically assume that the frozen carbon is located in the upper permafrost above 3 meters depth
55 and below the maximum ALT (Koven et al., 2011; Schaefer et al., 2011; MacDougall et al.,
56 2012). Thus, the simulated ALT determines the volume of permafrost in the top 3 meters of soil,
57 and thus the initial amount of frozen carbon. Consequently, any biases in the simulated ALT
58 will influence the initial amount of frozen carbon, even if different models initialize the frozen
59 carbon in the same way. Also, the same thermal biases that lead to deeper simulated active
60 layers also lead to warmer soil temperatures, making the simulated permafrost more vulnerable
61 to thaw and resulting in higher emissions estimates (Koven et al., 2013).

62 The surface organic layer (SOL) is the surface soil layer of nearly pure organic matter

Kevin Schaefer 2/2/2016 11:29 AM

Deleted: about

Elchin Jafarov 1/30/2016 11:01 AM

Deleted: i

Kevin Schaefer 2/1/2016 10:30 AM

Deleted: area and

66 that exerts a huge influence on the thermodynamics of the active layer. The organic layer
67 thickness (OLT) usually varies between 5-30 cm, depending on a balance between the litter
68 accumulation rate relative to the organic matter decomposition rate (Yi et al., 2009; Johnstone et
69 al., 2010). A recent model intercomparison study shows that LSMs need more realistic surface
70 processes such as a SOL and better representations of subsoil thermal dynamics (Ekici et al.,
71 2014a). The low thermal conductivity of the SOL makes it an effective insulator, decreasing the
72 heat exchange between permafrost and the atmosphere (Rinke et al., 2008). The effect of the
73 SOL has been well presented in several modeling studies. For example, Lawrence and Slater
74 (2008) showed that soil organic matter affects the permafrost thermal state in the Community
75 Land Model (CLM), and Jafarov et al., (2012) discussed the effect of the SOL in the regional
76 modeling study for Alaska, United States. Recently, Chadburn et al., (2015a,b) incorporated a
77 SOL in the Joint UK Land Environment Simulator (JULES) model to illustrate its influence on
78 ALT and ground temperatures both at a site specific study in Siberia, Russia, and globally. In
79 essence, the soil temperatures and ALT decrease as the OLT increases. Consequently, how (or
80 if) LSMs represent the SOL in the simulated soil thermodynamics will simultaneously determine
81 the initial amount of frozen permafrost carbon and the vulnerability of the simulated permafrost
82 to thaw.

83 In this study we improved present day frozen carbon stocks in the Simple
84 Biosphere/Carnegie-Ames-Stanford Approach (SiBCASA) model to reduce biases in initial
85 permafrost carbon stocks and improve the dynamics of future permafrost carbon release. To
86 achieve this we introduced three improvements into the SiBCASA model: 1) improve the soil
87 thermal dynamics and ALT, 2) improve soil carbon dynamics and build-up of carbon stocks in
88 soil, and 3) initialize the older, frozen carbon using observed circumpolar soil carbon (Hugelius

Kevin Schaefer 2/2/2016 11:33 AM

Deleted: the

Kevin Schaefer 2/2/2016 11:34 AM

Deleted: the

Kevin Schaefer 2/2/2016 11:35 AM

Deleted: of

Elchin Jafarov 1/30/2016 11:12 AM

Deleted: in simulations

Elchin Jafarov 1/30/2016 11:01 AM

Deleted: i

94 et al., 2014).

95

96 **2. Methods**

97 We used the SiBCASA model (Schaefer et al., 2008) to evaluate current soil carbon
98 stocks in permafrost affected soils. SiBCASA has fully integrated water, energy, and carbon
99 cycles and computes surface energy and carbon fluxes at 10 minute time steps. SiBCASA
100 predicts the moisture content, temperature, and carbon content of the canopy, canopy air space,
101 and soil (Sellers et al., 1996a; Vidale and Stockli, 2005). To calculate plant photosynthesis, the
102 model uses a modified Ball-Berry stomatal conductance model (Ball, 1998; Collatz et al., 1991)
103 coupled to a C3 enzyme kinetic model (Farquhar et al., 1980) and a C4 photosynthesis model
104 (Collatz et al., 1992). It predicts soil organic matter, surface litter, and live biomass (leaves,
105 roots, and wood) in a system of 13 prognostic carbon pools as a function of soil depth (Schaefer
106 et al., 2008). The model biogeochemistry does not account for disturbances, such as fire, and
107 does not include a nitrogen cycle. SiBCASA separately calculates respiration losses due to
108 microbial decay (heterotrophic respiration) and plant growth (autotrophic respiration).

109 SiBCASA uses a fully coupled soil temperature and hydrology model with explicit
110 treatment of frozen soil water originally from the Community Climate System Model, Version
111 2.0 (Bonan, 1996; Oleson et al., 2004). To improve simulated soil temperatures and permafrost
112 dynamics, Schaefer et al. (2009) increased the total soil depth to 15 m and added the effects of
113 soil organic matter on soil physical properties. Simulated snow density and depth, and thus
114 thermal conductivity, significantly influence simulated permafrost dynamics, so Schaefer et al.
115 (2009) added the effects of depth hoar and wind compaction on simulated snow density and
116 depth. Recent model developments include accounting for substrate availability in frozen soil

117 biogeochemistry (Schaefer and Jafarov, 2015).

118 We spun SiBCASA up to steady-state initial conditions using an input weather dataset
119 from the modified Climatic Research Unit National Center for Environmental Predictions
120 (CRUNCEP)¹ (Wei et al, 2014) for the entire permafrost domain in the northern hemisphere
121 (Brown et al., 1997). CRUNCEP is modeled weather data at 0.5x0.5 degree latitude and
122 longitude resolution optimally consistent with a broad array of observations. The CRUNCEP
123 dataset used in this study spans 110 years, from 1901 to 2010. We selected the first 30 years
124 from the CRUNCEP dataset (1901 to 1931) and randomly distributed them over 900 years. To
125 run our simulations we used JANUS High Performance Computing (HPC) Center at University
126 of Colorado at Boulder. The 900-yr time span was chosen in order to make optimal use of the
127 computational time, which allowed us to finish one spinup simulation on JANUS HPC without
128 interruptions.

129

130 2.1. Frozen carbon initialization

131 We initialized the frozen carbon stocks using the Northern Circumpolar Soil Carbon
132 Dataset version 2 (NCSCDv2) (Hugelius et al., 2014). The NCSCDv2 includes soil carbon
133 density maps in permafrost-affected soils available at several spatial resolutions ranging from
134 0.012° to 1°. The dataset consists of spatially extrapolated soil carbon data from more than 1700
135 soil core samples. This dataset has three layers, each 1 meter in depth, distributed between
136 ground surface and 3 meter depth.

137 We placed the frozen carbon within the top three meters of simulated permafrost,
138 ignoring deltaic and loess deposits that are known to extend well beyond 3 meters of depth

¹ ftp://nacp.ornl.gov/synthesis/2009/frescati/temp/land_use_change/original/readme.htm

Elchin Jafarov 1/30/2016 11:04 AM

Deleted: i

Kevin Schaefer 2/2/2016 11:38 AM

Deleted: main

141 (Hugelius et al., 2014). The bottom of the permafrost carbon layer is fixed at 3 meters, while the
142 top varies spatially depending on the simulated ALT during the spinup run. We initialized the
143 permafrost carbon by assigning carbon from the NCSCDv2 to the frozen soil carbon pools below
144 the maximum thaw depth. These frozen pools remained inactive until the layer thaws.

145 We initialized frozen carbon between the permafrost table and 3 meters depth using two
146 scenarios: 1) spatially uniform distribution of the frozen carbon throughout the permafrost
147 domain (Schaefer et al., 2011), and 2) observed distribution of the frozen carbon according to the
148 NCSCDv2. It is important to know the “stable” depth of the active layer before initializing
149 frozen carbon. We run the model for several years in order to calculate ALT, and then initialized
150 frozen carbon below the maximum calculated ALT. The frozen carbon was initialized only once
151 after the first spinup simulation. For the next simulation we used the previously calculated
152 permafrost carbon. We defined an equilibrium point when changes in overall permafrost carbon
153 were negligible or almost zero.

154 The total initial frozen carbon in each soil layer between the permafrost table and 3
155 meters is

$$156 \quad C_{fr}^i = \rho_c \Delta z_i, \quad (1)$$

157 where C_{fr}^i is the total permafrost carbon within the i^{th} soil layer, ρ_c is the permafrost carbon
158 density, and Δz_i is the thickness of the i^{th} soil layer in the model. For the uniform permafrost
159 carbon distribution, spatially and vertically uniform ρ_c of 21 kg C m⁻³ (Schaefer et al., 2011).
160 For the observed distribution from the NCSCDv2, ρ_c varies both with location and depth
161 (Hugelius et al., 2013).

162 The permafrost carbon in each layer is divided into three soil carbon pools as follows:

Kevin Schaefer 2/2/2016 11:39 AM
Deleted: during
Kevin Schaefer 2/2/2016 11:39 AM
Deleted: equilibrium run cycle
Kevin Schaefer 2/2/2016 11:40 AM
Deleted: equilibrium run

Kevin Schaefer 2/2/2016 11:41 AM
Deleted: $\rho_c = 21$ kg
Kevin Schaefer 2/2/2016 11:41 AM
Deleted: and assumed to be spatially and vertically uniform
Elchin Jafarov 1/30/2016 11:04 AM
Deleted: i

$$\begin{aligned} C_{slow}^i &= 0.8C_{fr}^i \\ C_{met}^i &= 0.2f_{root2met}C_{fr}^i \\ C_{str}^i &= 0.2f_{root2str}C_{fr}^i \end{aligned} \quad (2)$$

171 where $f_{root2met}$ and $f_{root2str}$ are the simulated fractions of root pool losses to the soil metabolic
172 and structural pools respectively (Schaefer et al., 2008). The nominal turnover time is 5 years
173 for the slow pool, 76 days for the structural pool, and 20 days for the metabolic pool. Schaefer et
174 al., (2011) has a 5% loss to the metabolic pool and a 15% loss to the structural pool based on
175 observed values in Dutta et al., (2006). The simulated fractions are actually 5.6% to the
176 metabolic pool and 14.4% to the structural pool. We found it encouraging that the numbers
177 calculated with the SiBCASA metabolic fractions resulted in numbers that are close to the
178 observed values in Dutta et al., (2006).

179

180 **2.2. Dynamic SOL**

181 We modified SiBCASA to include a dynamic SOL by incorporating the vertical
182 redistribution of organic material associated with soil accumulation. SiBCASA calculates the soil
183 physical properties as a weighted average of those for organic matter, mineral soil, ice and water
184 (Schaefer et al., 2009). The physical properties include soil porosity, hydraulic conductivity,
185 heat capacity, thermal conductivity, and matric potential. The model calculates the organic
186 fraction used in the weighted mean as the ratio of simulated carbon density to the density of pure
187 organic matter. The model does not account for the compression of organic matter. Since the
188 prognostic soil carbon pools vary with depth and time, the organic fraction and the physical
189 properties all vary with time and depth. We only summarized these calculations here since the
190 calculations are covered in detail in Schaefer et al. (2009).

191 | As live, above-ground biomass in the model dies, carbon is transferred into the first layer
192 | as litter. Without the vertical redistribution we describe here to create a surface organic layer,
193 | the top layer of the model tended to accumulate carbon in excess of that expected for pure
194 | organic matter. To allow vertical movement and build up a SOL, we placed a maximum limit on
195 | the amount of organic material that each soil layer can hold. When the simulated carbon content
196 | exceeds this threshold, the excess carbon is transferred to the layer below. This is a simplified
197 | version of the Koven et al., (2009) carbon diffusion model, which accounts for all sedimentation
198 | and cryoturbation processes. This simplified model is better suited for our application because
199 | we wanted to focus only to the buildup of a SOL.

Elchin Jafarov 1/30/2016 11:20 AM

Deleted: The previous version of the model distributed fine and coarse root growth vertically within the soil column based on observed root distributions. As the roots die, carbon is transferred to the soil carbon pools for that layer. Thus, the maximum rooting depth determined the maximum depth of 'current' or 'active' carbon in the model. Of course, if the maximum rooting depth fell below the permafrost table, the model would accumulate permafrost carbon, which remains inactive until the layer thaws.

200 | We calculate the maximum allowed carbon content per soil layer, C_{max} , as

$$201 \quad C_{max} = \rho_{max} \Delta z \frac{1000}{MW_C}, \quad (3)$$

202 | where ρ_{max} is the density of pure organic matter or peat, Δz is the soil layer thickness (m), MW_C
203 | is the molecular weight of carbon (12 g mol⁻¹), and the factor of 10³ converts from grams to
204 | kilograms. Based on observations of bulk densities of peat, we assume ρ_{max} is 140 kg m⁻³
205 | (Price et al., 2005). The MW_C term converts the expression into mol C m⁻², the SiBCASA
206 | internal units for carbon. The simulated organic soil fraction per soil layer, f_{org} , is defined as

$$207 \quad f_{org} = \frac{C}{C_{max}}, \quad (4)$$

208 | where C is the carbon content per soil layer (mol m⁻²). To convert to carbon we assume that the
209 | fraction of organic matter is 0.5, which means that half of the organic matter by mass is carbon.
210 | The original formulation allowed f_{org} to exceed 1.0 such that the excess organic material was
211 | essentially 'compressed' into the top soil layer, resulting in a 2-cm simulated SOL. We place an

Kevin Schaefer 2/2/2016 11:46 AM

Deleted: limit our model

224 upper limit of 0.95 on f_{org} and transfer the excess carbon to the layer below. The OLT is
225 defined as the bottom of the lowest soil layer where f_{org} is 0.95.

226

227

228 **2.3. Coupling growth to thaw depth**

229 We coupled simulated gross primary productivity (GPP), plant phenology, and root
230 growth to simulated thaw depth as a function of time. The model assumes root growth decreases
231 exponentially with depth based on observed vertical root distributions (Jackson et al., 1996;
232 Schaefer et al., 2008). The maximum rooting depth for completely thawed soil is defined as the
233 soil depth corresponding to 99% of the observed vertical root distribution or 1.1 m for the tundra
234 and boreal forest biomes. In real life, growing roots cannot penetrate frozen soil, so we restricted
235 simulated root growth to occur only within the thawed portion of the active layer (Tryon and
236 Chapin 1983, Van Cleve et al., 1983). The date of snowmelt determines the start date of the
237 growing season and the start of active layer thawing (Grøndahl et al. 2007; Wipf and Rixen
238 2010). Since fine root and leaf growth are coupled (Schaefer et al., 2008), constraining root
239 growth to thawed soil also constrains spring leafout to occur after the active layer starts thawing.
240 In real life plants cannot photosynthesize without liquid water in the soil, so we scaled simulated
241 GPP based on the fraction of thawed roots in the root zone.

242 The previous version of the model distributed fine and coarse root growth vertically
243 within the soil column based on observed root distributions. As the roots died, carbon was
244 transferred to the soil carbon pools for that layer. Thus, the maximum rooting depth determined
245 the maximum depth of 'current' or 'active' carbon in the model. Of course, if the maximum

Kevin Schaefer 2/2/2016 11:51 AM
Deleted: is

247 rooting depth fell below the permafrost table, the model would incorrectly grow roots directly
248 into frozen soil and consequently accumulate permafrost carbon.

Kevin Schaefer 2/2/2016 11:53 AM

Deleted: , which remains inactive until the layer thaws

249 In order to restrict simulated root growth to thawed soil layers, we first calculated the
250 fraction of thawed roots within the root zone defined by:

Elchin Jafarov 1/30/2016 11:23 AM

Deleted: We restricted simulated root growth to occur only in thawed soil layers. In SiBCASA, leaf growth is linked to fine root growth (Schaefer et al., 2008), so this also delays spring leafout until the soil begins to thaw. We first calculated the fraction of thawed roots within the root zone defined by

$$251 \quad R_{th} = \sum_{i=1}^{n_{root}} R_{f_i} (1 - F_{ice_i}), \quad (6)$$

252 where R_{th} is the fraction of total roots that are thawed, n_{root} is the soil layer corresponding to the
253 maximum root depth, R_{f_i} is the reference root fraction for the i^{th} soil layer based on observed
254 root distributions, and F_{ice_i} is the ice fraction calculated from the simulated ice content for the i^{th}
255 soil layer. When R_{th} equals one, the entire root zone is thawed and when R_{th} is zero, the entire
256 root zone is frozen. We assume evenly distributed liquid water in each layer such that F_{ice} equals
257 the frozen soil fraction. We then calculated R_{eff_i} , the effective root fraction for the i^{th} soil layer,

$$258 \quad R_{eff_i} = R_{f_i} (1 - F_{ice_i}) / R_{th}. \quad (7)$$

259 We then use R_{eff_i} to distribute new fine and coarse root growth within the soil column. When
260 R_{eff_i} equals zero, the soil layer is frozen with no root growth. Dividing by R_{th} ensures R_{eff_i}
261 sums to one within the soil column to conserve mass. This formulation makes the effective
262 maximum rooting depth equal to the thaw depth.

263 To couple GPP to thaw depth, we treated the reference root zone distribution for
264 completely thawed soil as the maximum root growth capacity defining the maximum potential
265 GPP. When $R_{th} < 1$, the root zone is partially frozen and GPP is less than its full potential. We
266 defined a GPP scaling factor, $S_{soilfrz}$, as

275
$$S_{soilfrz} = \begin{cases} R_{th} & \text{for } R_{th} \geq 0.01 \\ 0 & \text{for } R_{th} < 0.01 \end{cases} \quad (8)$$

276 This assumes that at least 1% of the roots must be thawed for GPP to occur, corresponding to
277 about ~1 cm of thawed soil. $S_{soilfrz}$ is applied along with the drought stress and temperature
278 scaling factors to constrain photosynthesis (Schaefer et al., 2008). SiBCASA assumes that the
279 factors that control GPP also control wood and leaf growth, so we also included $S_{soilfrz}$ as a new
280 scaling factor in addition to the drought stress and temperature scaling factors that control wood
281 and leaf growth.

282

283 **3. Results**

284 The dynamic SOL decreased the simulated ALT on average 50% across the domain and
285 allowed the model to simulate permafrost in discontinuous zones where it could not before
286 (Figure 1). The area of near surface permafrost simulated with the current version of the model
287 equals to 13.5 mil km² which is almost 38% greater than without the dynamic SOL (Schaefer et
288 al., 2011). This area is closer to the observed area from the International Permafrost Association:
289 16.2 mil km² (Brown et al., 1997). Simulated ALT less than 2 m covers about 92% of the area in
290 the new simulations (Figure 1B) in comparison to 66% of the area in the Schaefer et al. (2011)
291 simulations (Figure 1A). The previous version of SiBCASA could not simulate permafrost in
292 many parts of the discontinuous zone with relatively warm climate. Adding the dynamic SOL
293 essentially decreased the thermal conductivity of the surface soil allowing SiBCASA to simulate
294 permafrost where the mean annual air temperatures (MAAT) are close to 0 °C.

295 To illustrate the improvement of the simulated ALT with respect to the observed data, we
296 compared simulated ALT with measured values from Circumpolar Active Layer Monitoring

297 (CALM) stations. The CALM network is a part of the Global Terrestrial Network for Permafrost
298 (GTN-P) (Burgess et al., 2000). The monitoring network measures ALT either using a
299 mechanical probe or a vertical array of temperature sensors (Brown et al., 2000; Shiklomanov et
300 al., 2010). After matching up the CALM coordinates with the coordinates of previously
301 simulated ALT (Schaefer et al., 2011), we excluded sites with no measurements or ALT greater
302 than 3m depth, ending up with 76 CALM stations. Figure 2 shows simulated vs. observed ALT
303 for the 76 CALM sites. The current simulations have a higher resolution than Schaefer et al.
304 (2011) simulations, which allowed us to reach a higher order of heterogeneity between measured
305 and simulated ALTs. The Pearson's correlation coefficient, R , is negative and not significant for
306 the Schaefer et al. (2011) simulations (Figure 2A), but is positive and statistically significant for
307 the current simulations assuming $p < 0.05$ (Figure 2B). The dynamic SOL greatly improves the
308 simulated ALT, but SiBCASA still tends to overestimate ALT.

309 Figure 3 illustrates the effect of the frozen soil restrictions on phenology and GPP at a
310 single point in central Siberia. Before applying a frozen soil restriction, SiBCASA maintained
311 fine roots even in winter, resulting in root growth all year with a peak in spring corresponding to
312 simulated leafout (Figure 3A). Simulated GPP was restricted by liquid water availability and
313 was closely tied to thawing of the active layer, resulting in a lag as high as 60 days between
314 leafout and start of GPP in spring. Restricting growth and GPP to when the soil is thawed
315 essentially synchronizes all phenological events to occur at the same time (Figure 3B).

316 Restricting growth and GPP to when the soil is thawed delayed the onset of plant
317 photosynthesis in spring in permafrost-affected regions. Introduction of the thawed root fraction
318 in the model reduced GPP primarily in early spring. To illustrate the difference between
319 unconstrained and restricted root growth (Figure 3), we ran the model for ten years for both

320 cases. The difference between unconstrained and restricted root growth resulted in an overall
321 ~9% reduction in annual GPP for the entire permafrost domain, nearly all of which occurred in
322 spring.

323 To illustrate soil carbon distribution with depth we selected three representative areas: a
324 continuous permafrost area corresponding to tundra type biome above the Arctic Circle, an area
325 in the boundary of continuous and discontinuous permafrost corresponding to the boreal forest
326 biome, and an area near the south border of the discontinuous permafrost corresponding to
327 poorly vegetated-rocky areas. We calculated the mean and standard deviation of the carbon
328 density distribution with depth for 200 grid points around each of the three selected locations.
329 Simulated typical carbon densities from the selected locations are shown on Figure 4. All
330 profiles shown on Figure 4 show a similar pattern: a 20-30 cm SOL with reduced carbon content
331 at the bottom of the active layer. The SOL and permafrost carbon content matches observed
332 values (Harden et al., 2012), but carbon content near the bottom of the active layer does not,
333 most likely because our model does not include cryoturbation processes.

334 The decrease in ALT resulting from a dynamic SOL increases the volume of permafrost
335 in the top 3 meters of soil, greatly increasing the initial amount of frozen permafrost carbon in
336 the simulations. Schaefer et al. (2011) without the dynamic SOL assumed a uniform permafrost
337 carbon density of $21 \text{ kg} \cdot \text{C} \cdot \text{m}^{-3}$, resulting in a total of 313 Gt of permafrost carbon at the start
338 of their transient run (Figure 5A). To compare with the Schaefer et al. [2011] results, we
339 initialized the permafrost carbon using the same assumed uniform carbon density and ran
340 SiBCASA to steady state initial conditions (Figure 5B). Assuming the same uniform carbon
341 density, the current version with the dynamic SOL results in a total of ~680 Gt C compared to
342 313 Gt C in Schaefer et al. (2011). The dynamic SOL effectively doubled the volume of

343 permafrost in the top three meters of soil and the amount of simulated frozen carbon.

344 Initializing SiBCASA with the observed spatial distribution of permafrost carbon from
345 the NCSCDv2 resulted in ~560 GtC of carbon stored in permafrost after spinup, close to the
346 observed value ~550 GtC in the top three meters of soil (Hugelius et al., 2014). This does not
347 mean that after the spinup simulated permafrost carbon stocks exactly matched the NCSDC data.
348 In discontinuous zones, for example, if the model simulated permafrost, it tended to produce a
349 deeper ALT and thus less permafrost carbon than the NCSCDv2. Assuming a uniform
350 permafrost carbon density does not account for the spatial heterogeneity in permafrost carbon
351 and overestimates the total amount of permafrost carbon compared to the NCSCDv2 (680 Gt C
352 vs. 550 Gt C). The spatial correlation between simulated and observed permafrost carbon is 0.63
353 when initializing with the NCSCDv2 (Fig 6b), compared with a spatial correlation of 0.12 for the
354 uniform permafrost carbon density (Fig 6a). The amount and spatial distribution of permafrost
355 carbon significantly improves when initializing with NCSCDv2.

Kevin Schaefer 2/2/2016 12:35 PM

Deleted: During spinup, ALT varies with time, introducing carbon movement from frozen to thawed pools.

Kevin Schaefer 2/2/2016 12:49 PM

Deleted: The major difference between uniform frozen carbon initialization (Fig 6A) and initialization using the NCSCD (Fig 6B) is that SiBCASA simulated permafrost in more places. However, the NCSCD map (Fig 6B) shows that not all permafrost regions contain a uniform amount of frozen carbon. Therefore simulating 'correct' ALT is important and should improve the overall permafrost carbon storage.

357 4. Discussion

358 Failure to simulate soil carbon in southeast Canada and southwest Siberia (Figure 6C) is
359 attributed to deep ALT. These areas correspond to the peat lands. Our model uses Harmonized
360 World Soil Carbon Database (HWSD) (FAO et al., 2009) to initialize soil texture and related
361 thermal properties. Deep layers of peat have low thermal conductivities providing an ideal
362 condition for permafrost existence. However, The HWSD does address peat lands in southeast
363 Canada and southwest Siberia.

Kevin Schaefer 2/2/2016 12:04 PM

Deleted: active layer thickness

377 | The overestimation of SOC in Central Siberia results from coupling between GPP and
378 | ALT. The dynamic SOL and rooting depth strengthens the feedback between GPP and ALT
379 | (Koven et al., 2009). Higher GPP produces greater litter fall, which increases the input soil
380 | carbon at the surface and results in a thicker SOL. The dynamic SOL changes the properties of
381 | the near surface soil, resulting in a shallower ALT and cooler soil temperatures. The dynamic
382 | rooting depth accounts for a shallower ALT and modulates GPP accordingly. The cooler soil
383 | temperatures slow microbial decay and increase the carbon accumulation rate, which in turn
384 | increases the SOL and reduces ALT further. Eventually, this feedback results in the
385 | development of a peat bog. The changes we describe here indicate that SiBCASA can simulate
386 | the dynamics of peat bog development, but the model does not yet include a dynamic vegetation
387 | model to account for conversions between biome types, such as boreal forest to peat bog.

388 | The overall amount of permafrost carbon is less than that calculated assuming a uniform
389 | frozen carbon distribution. It is important to note that the SOL, ALT, and the permafrost
390 | thickness are the same for both cases (Figure 6A and B). This is due to the fact that in both cases
391 | soil carbon is added in the permafrost layer below the active layer. Consequently, the ALT does
392 | not change between simulations and the volume of permafrost in the top three meters of soil does
393 | not change as well. The smaller permafrost carbon stock simulated for the non-uniform case is
394 | mainly due to the fact that we did not initialize frozen carbon in regions where according to the
395 | NCSCDv2 it is not present, such as the Brooks Range in Alaska.

396 | The dynamic SOL insulates ALT from air temperature, allowing SiBCASA to simulate
397 | permafrost in many discontinuous permafrost regions where it could not before, consistent with
398 | previous results where changes in thermal properties associated with the presence of soil organic
399 | matter cooled the ground (Lawrence and Slater, 2008; Yi et al., 2009; Ekici et al., 2014b;

Kevin Schaefer 2/2/2016 1:05 PM

Comment [1]: made active voice

Kevin Schaefer 2/2/2016 12:07 PM

Deleted: is a

Kevin Schaefer 2/2/2016 12:07 PM

Deleted: of

Elchin Jafarov 1/30/2016 11:38 AM

Deleted: the amount of soil carbon in

Elchin Jafarov 1/30/2016 11:40 AM

Deleted: active layer

Elchin Jafarov 1/30/2016 11:42 AM

Deleted: r

Kevin Schaefer 2/2/2016 12:15 PM

Deleted: has the same thermal and carbon dynamics, and thus AL-preserving permafrost distribution and thickness

Elchin Jafarov 1/30/2016 11:41 AM

Deleted: T.

Kevin Schaefer 2/2/2016 12:17 PM

Moved down [1]: (Lawrence and Slater, 2008; Yi et al., 2009; Ekici et al., 2014b; Chadburn et al., 2015a,b)

Kevin Schaefer 2/2/2016 12:17 PM

Deleted:), when

Kevin Schaefer 2/2/2016 12:17 PM

Moved (insertion) [1]

413 | [Chadburn et al., 2015a,b](#)). In addition, our work confirms findings by Koven et al., (2009)
414 showing that including SOL dynamics into the model improves agreement with the observed
415 permafrost carbon stocks. However, to better simulate known permafrost distribution in the
416 discontinuous permafrost zone it is important to know the exact OLT. Unfortunately, in situ
417 measurements of OLT are scarce and essentially lacking in most areas of continuous and
418 discontinuous permafrost.

419 To investigate further the influence of the environmental factors on ALT we looked at the
420 relationship between ALT and near surface air temperatures (NSAT), soil wetness fraction
421 (SWF), down-welling long-wave radiation (DLWR), and snow depth (SD). The simulated ALT
422 is most influenced by NSAT and soil SWF, with a slightly smaller influence by DLWR, and
423 nonlinearly influenced by SD (Figure 7). To show the influence of the NSAT we averaged two
424 early fall months over 10 years. The areas with deep simulated ALT correspond to annual
425 NSAT > 1° C in southwest Siberia and NSAT > 5° C in the southeast Canada with a statistically
426 significant correlation of 0.62 (Figure 7A). DLWR showed a similar, but slightly weaker
427 relationship with ALT, with deeper ALT in southeast Canada and southwest Siberia and
428 statistically significant correlation of 0.45 (Figure 7B). Figure 7C shows maximum simulated
429 snow depth calculated over the last 10 years of the steady state run. Our results show no
430 correlation between SD and ALT, but the effects of snow on ALT are less obvious and depend
431 on different physical processes, such as wind, snow metamorphism, and depth hoar formation
432 (Sturm et al., 1997; Ekici et al., 2014; Jafarov et al., 2014). Zhang (2005) indicates that SD less
433 than 50cm have the greatest impact on soil temperatures. We also observe high SWF in
434 southwest Siberia and southeast Canada (see Figure 7D) where SiBCASA simulates deep ALT

435 with a statistically significant correlation of 0.68, suggesting wet soils modulate the insulating
436 effects of the SOL (Lawrence and Slater, 2008).

437 This work does not address the fire impacts on soil thermodynamics and recovery from
438 fire, both of which are strongly influenced by the changes in the SOL (Jafarov et al., 2013).
439 Studies show that wildfires and climate change could substantially alter soil carbon storage
440 (Yuan et al., 2012; Yi et al., 2010). In the current version of the model the topsoil carbon stays
441 in the system and provides resilience to permafrost. However, in reality, the upper SOL could be
442 removed by fire, which would alter soil thermal properties and perturb permafrost carbon
443 stability.

444

445 5. Conclusion

446 This work shows the dynamic organic layer directly improves the distribution of carbon
447 in soil, as well as indirectly through the improved ALT. Initialization of the carbon according to
448 the NCSCDv2 map allowed us to better match with the observed carbon distribution. Restriction
449 of the root growth within the thawed layer prevented artificial accumulation of permafrost
450 carbon. Our model developments improved both the total amount and the spatial distribution of
451 simulated permafrost carbon. The total permafrost carbon increasing from 313 Gt C to 560 Gt C,
452 compared to the observed value of 550 Gt C, and the spatial correlation with the observed
453 distribution increased from 0.12 to 0.63. These improvements indicate the importance of
454 including these developments in all land surface models.
455 In addition, most of the LSMs calculate soil properties based on prognostic soil carbon and soil
456 texture from HWSD. We found that HWSD does not include thermal properties of peat lands,

Kevin Schaefer 2/2/2016 12:24 PM

Deleted: model from

Kevin Schaefer 2/2/2016 12:54 PM

Deleted: As a result of the model developments we improved the spatial distribution of the permafrost carbon by more than 50% as well as storage by ~259 GtC.

Elchin Jafarov 2/2/2016 3:17 PM

Deleted: M

463 which resulted in inaccurate modeling of the ALT at the southern boundaries of the permafrost
464 domain in Canada and Russia.

Elchin Jafarov 2/2/2016 3:16 PM

Deleted: We suggest modifying the HWSO to better address thermal properties of the peat lands

465 6. Acknowledgements

466 This research was funded by NOAA grant NA09OAR4310063 and NASA grant NNX10AR63G.
467 This work utilized the Janus supercomputer, which is supported by the National Science
468 Foundation (award number CNS-0821794) and the University of Colorado Boulder. We thank
469 K. Gregory at NSIDC for reviewing the manuscript. Software tools used in this study include
470 m_map MATLAB package and shadedErrorBar.m MATLAB script.

471

472 7. References

473 Ball, J. T.: An analysis of stomatal conductance, Ph.D. thesis, Stanford Univ., Stanford, Calif.,
474 1988

475 Bonan, G. B.: A Land Surface Model (LSM Version 1.0) for ecological, hydrological, and
476 atmospheric studies: Technical description and users guide, NCAR Tech. Note
477 NCAR/TN-417+STR, Natl. Cent. for Atmos. Res., Boulder, Colo., 1996.

478 Brown, J., K. Hinkel and F. Nelson.: The 1 Circumpolar Active Layer Monitoring (CALM)
479 program: Research designs and initial results. *Polar Geography*, 24,165-258,
480 doi:10.1080/10889370009377698. 2000.

481 Brown, J., O. J. Ferrians Jr., J. A. Heginbottom, and E. S Melnikov, Eds.: Circum-Arctic Map of
482 Permafrost and Ground-Ice Conditions. U.S. Geological Survey in Cooperation with the
483 Circum-Pacific Council for Energy and Mineral Resources, Circum-Pacific Map Series

486 CP-45, scale 1:10,000,000, 1 sheet, 1997

487 Brown, J., Hinkel, K.M.; Nelson, F.E.: The circumpolar active layer monitoring (CALM)
488 program: Research designs and initial results. *Polar Geog.*, 24, 165–258, 2000.

489 Bonan, G. B.: A Land Surface Model (LSM Version 1.0) for ecological, hydrological, and
490 atmospheric studies: technical description and users guide. NCAR Technical Note
491 NCAR/TN-417+STR, Boulder, Colorado. 1996.

492 Burgess, M.M.; Smith, S.L.; Brown, J.; Romanovsky, V.; Hinkel, K. The Global Terrestrial
493 Network for Permafrost (GTNet-P): Permafrost Monitoring Contributing to Global
494 Climate Observations. Available online:
495 http://ftp2.cits.rncan.gc.ca/pub/geott/ess_pubs/211/211621/cr_2000_e14.pdf.

496 Burke, EJ, IP Hartley, and CD Jones.: Uncertainties in the global temperature change caused by
497 carbon release from permafrost thawing, *Cryosphere*, 6, 1063–1076, doi:10.5194/tc-6-
498 1063-2012, 2012

499 Camill, P: Permafrost thaw accelerates in boreal peatlands during late-20th century climate
500 warming *Clim. Change* 68 135–52. 2005

501 Callaghan, T.V., Johansson, M., Anisimov, O., Christiansen, H.H., Instanes, A., Romanovsky,
502 V., and Smith, S.: Chapter 5: Changing permafrost and its impacts. In: *Snow, Water, Ice
503 and Permafrost in the Arctic (SWIPA) 2011. Arctic Monitoring and Assessment
504 Programme (AMAP), Oslo, pp 62. 2011.*

505 Chadburn, S., Burke, E., Essery, R., Boike, J., Langer, M., Heikenfeld, M., Cox, P., and
506 Friedlingstein, P.: An improved representation of physical permafrost dynamics in the
507 JULES land surface model, *Geosci. Model Dev. Discuss.*, 8, 715–759,

508 doi:10.5194/gmdd-8-715-2015, 2015a.

509 Chadburn, S. E., Burke, E. J., Essery, R. L. H., Boike, J., Langer, M., Heikenfeld, M.,
510 Cox, P. M., and Friedlingstein, P.: Impact of model developments on present and future
511 simulations of permafrost in a global land-surface model, *The Cryosphere Discuss.*, 9,
512 1965-2012, doi:10.5194/tcd-9-1965-2015, 2015b.

513 Collatz, G. J., J. T. Ball, C. Grivet, and J. A. Berry.: Physiological and environmental regulation
514 of stomatal conductance, photosynthesis, and transpiration: A model that includes a
515 laminar boundary layer, *Agric. For. Meteorol.*, 54, 107– 136, doi:10.1016/0168-
516 1923(91)90002-8, 1991.

517 Collatz, G. J., M. Ribascarbo, and J. A. Berry.: Coupled photosynthesis-stomatal conductance
518 model for leaves of C4 plants, *Aust. J. Plant Physiol.*, 19(5), 519–538, 1992.

519 Dutta, K., Schuur, E. A. G., Neff, J. C. and Zimov, S. A.: Potential carbon release from
520 permafrost soils of Northeastern Siberia. *Global Change Biol.* 12, 2336–2351, 2006.

521 FAO, IIASA, ISRIC, ISS-CAS, and JRC: Harmonized World Soil Database (version 1.1) FAO,
522 Rome, Italy and IIASA, Laxenburg, Austria, 2009.

523 Ekici, A., Chadburn, S., Chaudhary, N., Hajdu, L. H., Marmy, A., Peng, S., Boike, J., Burke, E.,
524 Friend, A. D., Hauck, C., Krinner, G., Langer, M., Miller, P. A., and Beer, C.: Site-level
525 model intercomparison of high latitude and high altitude soil thermal dynamics in tundra
526 and barren landscapes, *The Cryosphere Discuss.*, 8, 4959-5013, doi:10.5194/tcd-8-4959-
527 2014, 2014a.

528 Ekici, A., Beer, C., Hagemann, S., Boike, J., Langer, M., and Hauck, C.: Simulating high-
529 latitude permafrost regions by the JSBACH terrestrial ecosystem model, *Geosci. Model*

530 Dev., 7, 631-647, doi:10.5194/gmd-7-631-2014, 2014b.

531 Farquhar, G. D., S. von Caemmerer, and J. A. Berry.: A biochemical model of photosynthetic
532 CO₂ assimilation in leaves of C₃ species, *Planta*, 149, 78–90, doi:10.1007/BF00386231,
533 1980.

534 Grøndahl L, Friborg T, Soegaard H.: Temperature and snow-melt controls on interannual
535 variability in carbon exchange in the high Arctic. *Theor Appl Climatol* 88(1):111–125,
536 2007.

537 Harden, J. W., Koven, C., Ping, C., Hugelius, G., McGuire D. A., Camill, P., Jorgenson, T.,
538 Kuhry, P., Michaelson, G. J., O'Donnell, J.A., Schuur, E. A. G., Tarnocai C., Johnson,
539 K., Grosse, G.: et al. (2012), Field information links permafrost carbon to physical
540 vulnerabilities of thawing, *Geophys. Res. Lett.*, 39, L15704, doi:10.1029/2012GL051958.

541 Hugelius, G., Strauss, J., Zubrzycki, S., Harden, J. W., Schuur, E. A. G., Ping, C.-L.,
542 Schirmermeister, L., Grosse, G., Michaelson, G. J., Koven, C. D., O'Donnell, J. A.,
543 Elberling, B., Mishra, U., Camill, P., Yu, Z., Palmtag, J., and Kuhry, P.: Estimated stocks
544 of circumpolar permafrost carbon with quantified uncertainty ranges and identified data
545 gaps, *Biogeosciences*, 11, 6573–6593, doi:10.5194/bg-11-6573-2014, 2014.

546 Hugelius, G., Tarnocai, C., Broll, G., Canadell, J. G., Kuhry, P., and Swanson, D. K.: The
547 Northern Circumpolar Soil Carbon Database: spatially distributed datasets of soil
548 coverage and soil carbon storage in the northern permafrost regions, *Earth Syst. Sci.*
549 *Data*, 5, 3–13, doi:10.5194/essd-5-3-2013, 2013.

550 Jafarov E E, Marchenko S S and Romanovsky V E.: Numerical modeling of permafrost
551 dynamics in Alaska using a high spatial resolution dataset, *Cryosphere*, 6, 613–24, 2012.

552 Jafarov E.E., Nicolsky D.J., Romanovsky V.E., Walsh J.E., Panda S.K., Serreze M.C. 2014. The
553 effect of snow: How to better model ground surface temperatures. *Cold Regions Science*
554 *and Technology*, Volume 102, Pages 63-77, ISSN 0165-232X, doi:
555 10.1016/j.coldregions.2014.02.007.

556 Jafarov, E. E., Romanovsky V. E., Genet, H., McGuire A., D., Marchenko, S. S.: The effects of
557 fire on the thermal stability of permafrost in lowland and upland black spruce forests of
558 interior Alaska in a changing climate, *Environmental Research Letters*, 8, 035030, 2013.

559 Jackson, R. B., J. Canadell, J. R. Ehleringer, H. A. Mooney, O. E. Sala, and E. D. Schulze.: A
560 global analysis of root distributions for terrestrial biomes, *Oecologia*, 108, 389–411,
561 doi:10.1007/BF00333714, 1996.

562 Johnstone J F, Chapin F S III, Hollingsworth T N, Mack M C, Romanovsky V and Turetsky M.:
563 Fire, climate change, and forest resilience in interior Alaska *Can. J. For. Res.* 40 1302–12,
564 2010.

565 Koven, C., P. Friedlingstein, P. Ciais, D. Khvorostyanov, G. Krinner, and C. Tarnocai.: On the
566 formation of high-latitude soil carbon stocks: Effects of cryoturbation and insulation by
567 organic matter in a land surface model, *Geophys. Res. Lett.*, 36, L21501,
568 doi:10.1029/2009GL040150, 2009.

569 Koven, CD, B Ringeval, P Friedlingstein, P Ciais, P Cadule, D Khvorostyanov, G Krinner, and
570 C Tarnocai.: Permafrost carbon-climate feedbacks accelerate global warming, *Proc. Natl.*
571 *Acad. Sci. USA*, 108(36), 14769–14774, doi/10.1073/pnas.1103910108, 2011.

572 Koven, C.D., W.J. Riley, and A. Stern.: Analysis of permafrost thermal dynamics and response
573 to climate change in the CMIP5 earth system models. *J. Climate*. 26:1877–1900.

574 doi:10.1175/JCLI-D-12-00228.1, 2013.

575 Lawrence, D. M., and A. G. Slater.: Incorporating organic soil into a global climate model.
576 *Climate Dynamics* 30(2-3): 145-160, doi:10.1007/s00382-007-0278-1, 2008.

577 MacDougall, AH, CA Avis and AJ Weaver.: Significant contribution to climate warming from
578 the permafrost carbon feedback, *Nature Geosci.*, 5, 719-721, DOI: 10.1038/NGEO1573,
579 2012.

580 Oberman, N.G.: Contemporary Permafrost Degradation of Northern European Russia. In:
581 *Proceedings Ninth International Conference on Permafrost*. Vol. 2, 1305-1310 pp, 2008.

582 Oleson, K.W., Dai, Y., Bonan, G., Bosilovich, M., Dickinson, R., and coauthors.: Technical
583 description of the Community Land Model (CLM). NCAR Tech. Note, TN-461+STR,
584 174 pp, 2004.

585 Price, J. S., J. Cagampang, and E. Kellner.: Assessment of peat compressibility: is there an easy
586 way? *Hydro. Processes*, 19, 3469–3475, 2005.

587 Sellers, PJ, DA Randall, GJ Collatz, JA Berry, CB Field, DA Dazlich, C Zhang, GD Collelo, L
588 Bounoua.: A Revised Land Surface Parameterization of GCMs, Part I: Model
589 Formulation, *J. Clim.*, 9(4), 676-705, 1996.

590 Schaefer, K., Collatz, G. J., Tans, P., Denning, A. S., Baker, I. and co-authors. : The combined
591 Simple Biosphere/Carnegie-Ames-Stanford Approach (SiBCASA) Model. *J. Geophys.*
592 *Res.*, 113, doi:10.1029/2007JG000603, 2008.

593 Schaefer, K. and Jafarov, E.: A parameterization of respiration in frozen soils based on substrate
594 availability, *Biogeosciences Discuss.*, 12, 12027-12059, doi:10.5194/bgd-12-12027-2015,
595 2015.

596 Schaefer, K., T. Zhang, L. Bruhwiler, and A. P. Barrett.: Amount and timing of permafrost
597 carbon release in response to climate warming, *Tellus Series B: Chemical and Physical*
598 *Meteorology*, DOI: 10.1111/j.1600-0889.2011.00527.x, 2011.

599 Schaefer, K., Zhang, T., Slater, A. G., Lu, L., Etringer, A. and Baker, I.: Improving simulated
600 soil temperatures and soil freeze/thaw at high-latitude regions in the Simple
601 Biosphere/Carnegie-Ames-Stanford Approach model. *J. Geophys. Res.*, 114,
602 doi:10.1029/2008JF001125, 2009.

603 Schaefer, K, H Lantuit, VE Romanovsky, EAG Schuur, and R Witt .: The impact of the
604 permafrost carbon feedback on global climate, *Env. Res. Lett.*, 9, 085003 (9pp)
605 doi:10.1088/1748-9326/9/8/085003, 2014.

606 Shiklomanov, N.I.; Streletskiy, D.A.; Nelson, F.E.; Hollister, R.D.; Romanovsky, V.E.; Tweedie,
607 C.E.; Bockheim, J.G.; Brown, J. Decadal variations of active-layer thickness in moisture-
608 controlled landscapes, Barrow, Alaska. *J. Geophys. Res.* 115, G00I04, 2010.

609 E. A. G. Schuur, A. D. McGuire, C. Schädel, G. Grosse, J. W. Harden, D. J. Hayes, G. Hugelius,
610 C. D. Koven, P. Kuhry, D. M. Lawrence, S. M. Natali, D. Olefeldt, V. E. Romanovsky,
611 K. Schaefer, M. R. Turetsky, C. C. Treat and J. E. Vonk.: Climate change and the
612 permafrost carbon feedback. *Nature* 520, 171–179. doi:10.1038/nature14338, 2015.

613 Smith, S., and M.M. Burgess.: Ground Temperature Database for Northern Canada. Geological
614 Survey of Canada Open File Report No. 3954. 28 pages, 2000.

615 Tarnocai, C., Canadell, J. G., Schuur, E. A. G., Kuhry, P., Mazhitova, G. and Zimov, S.: Soil
616 organic carbon pools in the northern circumpolar permafrost region. *Global Biogeochem.*
617 *Cycles*, 23, doi:10.1029/2008GB003327, 2009.

618 Tryon, P., Chapin, F. III.: Tem- perature controls over root growth and root biomass in taiga
619 forest trees. *Can. J. For. Res.* 13:827-33, 1983.

620 Van Cleve, K.L., Oliver, L., Schlentner, R., Viereck, L. and Dyrness, C.T.:Productivity and
621 nutrient cycling in tiaga forest exosystems. *Can. J. For. Res.*, 13: 747-766, 1983.

622 Vidale, PL, R Stockli.: Prognostic canopy air space solutions for land surface exchanges, *Theor.*
623 *Appl. Climatol.*, 80, 245-257, 2005.

624 Yi S, Manies K, Harden J and McGuire A D.: Characteristics of organic soil in black spruce
625 forests: implications for the application of land surface and ecosystem models in cold
626 regions *Geophys. Res. Lett.* 36 L05501, 2009.

627 Yi, S., A. D. McGuire, E. Kasischke, J. Harden, K. L. Manies, M. Mack, and M. R. Turetsky
628 (2010), A Dynamic organic soil biogeochemical model for simulating the effects of
629 wildfire on soil environmental conditions and carbon dynamics of black spruce forests, *J.*
630 *Geophys. Res.*, 115, G04015, doi:10.1029/2010JG001302.

631 Yuan, F., S. Yi, A. D. McGuire, K. H. Johnsen, J. Liang, J. Harden, E. Kasischke, and W. Kurz
632 (2012), Assessment of historical boreal forest C dynamics in Yukon River Basin:
633 Relative roles of warming and fire regime change, *Ecol. Appl.*, 22, 2091-2109.

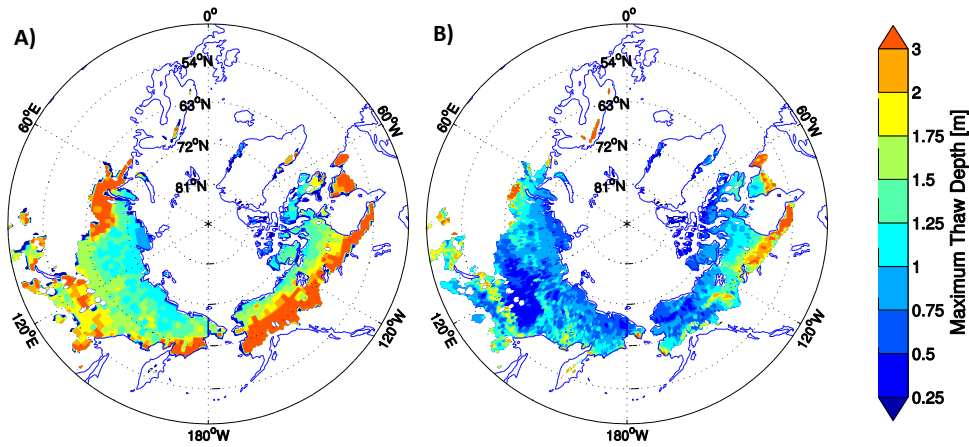
634

635 Wei, Y., Liu, S., Huntzinger, D. N., Michalak, A. M., Viovy, N., Post, W. M., Schwalm, C. R.,
636 Schaefer, K., Jacobson, A. R., Lu, C., Tian, H., Ricciuto, D. M., Cook, R. B., Mao, J., and
637 Shi, X.: The North American Carbon Program Multi-scale Synthesis and Terrestrial
638 Model Intercomparison Project: Part 2 - Environmental Driver Data. *Geoscientific Model*
639 *Development*, 7, 2875-2893, doi:10.5194/gmd-7-2875-2014, 2014.

640 Wipf, S., and Rixen, C.: A review of snow manipulation experiments in Arctic and alpine tundra
641 ecosystems. *Polar Res* 29(1):95–109. doi:10.1111/j.1751-8369.2010.00153.x, 2010.

642 Zhang, T.: Influence of the seasonal snow cover on the ground thermal regime: An overview,
643 *Rev. Geophys.*, 43, RG4002, doi:10.1029/2004RG000157, 2005.

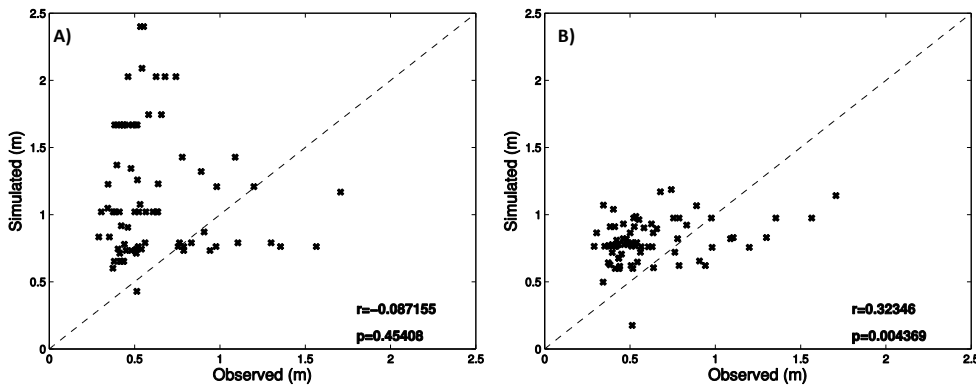
644



645

646 **Figure 1.** Maximum thaw depth (ALT) averaged over last five years after spinup from A) Schaefer et al.,
 647 (2011) and B) this study, in meters.

648

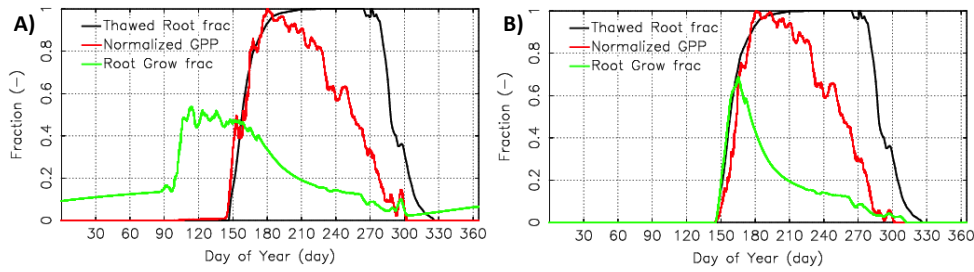


649

650 **Figure 2.** Comparison of ALT from 76 Circumpolar Active Layer Monitoring stations with the averaged
 651 ALT from last five years after spinup from A) Schaefer et al., (2011) and B) this study. r is a Pearson's
 652 correlation coefficient and p is a significance value, $p < 0.05$ stands for the 95% of confidence.

653

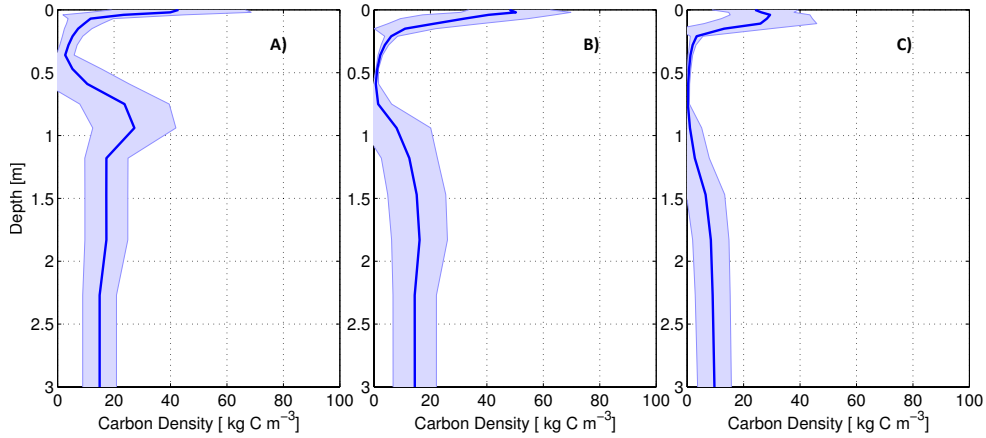
Kevin Schaefer 2/2/2016 12:56 PM
 Deleted: the mean active layer thickness (ALT)



655

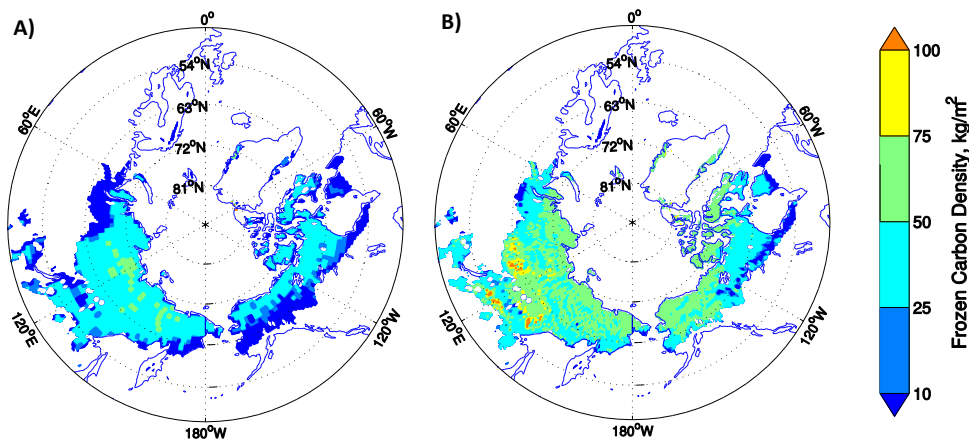
656 **Figure 3:** Root growth and GPP without (A) and with (B) the frozen soil constraint on growth. GPP is
 657 normalized to a maximum value of 1.0. The root growth fraction is relative to total plant growth.

Kevin Schaefer 2/2/2016 12:58 PM
 Deleted: A) and B) r



658

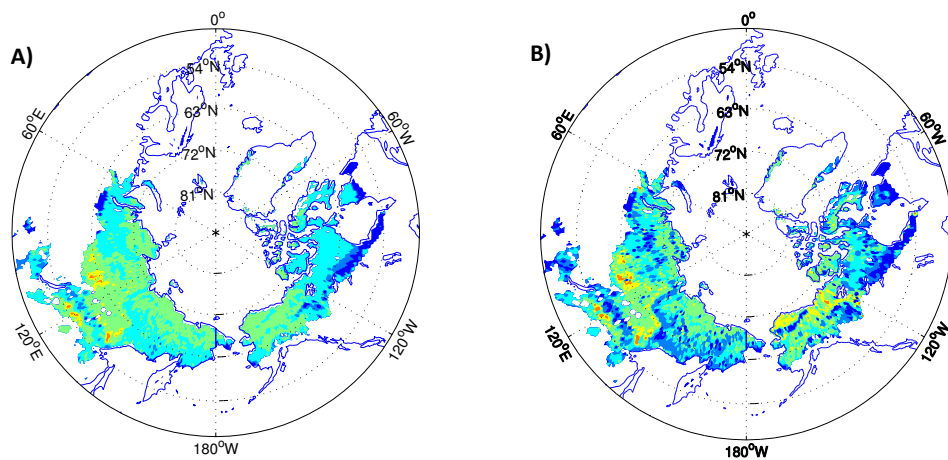
659 **Figure 4.** The average soil carbon distribution from 200 grid cells for A) a tundra region in continuous
 660 permafrost zone, B) boreal forest on the boundary between continuous and discontinuous zones, and C)
 661 low carbon soil at the south border of the discontinuous permafrost zone. The solid blue curve indicates
 662 the mean the white blue shading indicate the spread in the simulated soil carbon density.
 663



665

666 | **Figure 5.** The frozen carbon maps obtained assuming a uniform frozen carbon distribution at the initial
 667 time step, and averaged over five years at the end of the steady state run: A) from Schaefer et al., (2011),
 668 and B) from the current run, correspondingly.

669



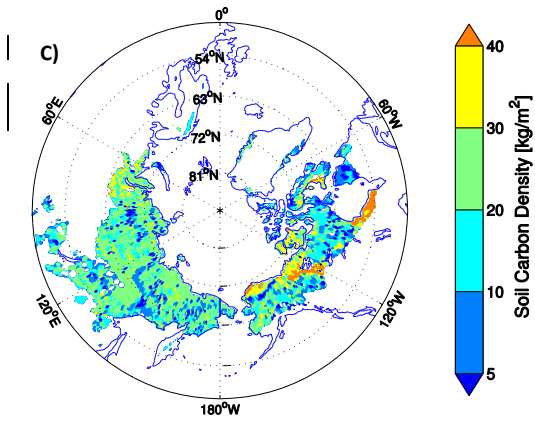
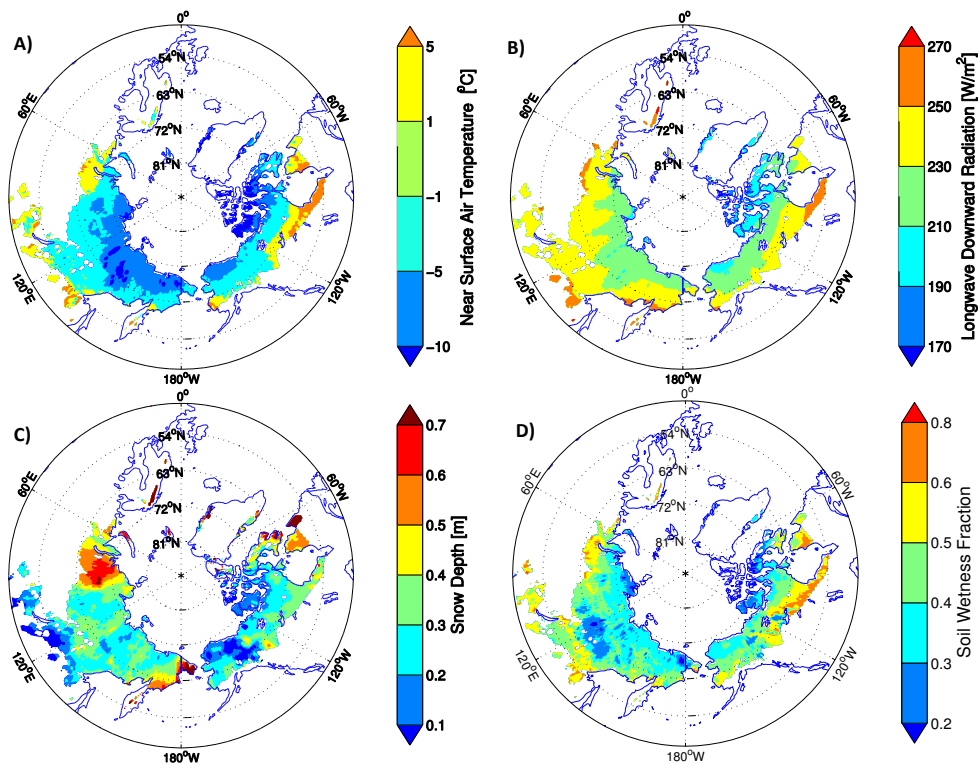


Figure 6. The soil carbon maps averaged over top 3 meters: A) from SiBCASA at the end of the steady state run with constant permafrost carbon density, B) from SiBCASA at the end of the steady state run with spatially varying permafrost carbon density, and C) from the NCSCDv2.

670

671



672

673 | **Figure 7.** A) The near-surface air temperature averaged over first two month of the fall season. B) The
 674 down-welling long-wave radiation, averaged yearly over 10 years. C) The maximum snow depth obtained
 675 over 10 years for the steady state run, and D) the soil wetness fraction (dimensionless fraction of 1),
 676 representing overall near-surface soil wetness, averaged yearly over 10 years.

677

678